

PSO-based Log-Gabor filter for Fringe Projection Profilometry

Jesús Pineda, Jhacson Meza, Juan Dominguez

Abstract—In Fourier Transform Profilometry, a filtering procedure is performed to separate the desired information (first order spectrum) from other unwanted contributions such as the background component (zero-order spectrum). However, if the zero-order spectrum and the high order spectra component interfere the fundamental spectra, the filtering procedure turn into a difficult task. To overcome this difficulty, in this work a new particle swarm optimization approach for filter modeling was developed to achieve more accurate extraction of the first-order spectrum in Fourier Transform Profilometry. The algorithm takes advantage of the adaptive nature of the Log-Gabor filters. Encouraging experimental results show the advantage of the proposed method.

I. INTRODUCTION

Fringe Projection Profilometry (FPP) is a widely used technique based on structured illumination for optical three-dimensional (3D) shape measurements. This method provides the 3D topography of objects in a non-contact manner, with high resolution, and fast data processing. In a typical FPP set-up, a fringe projector, and a camera are positioned in a triangulation-based arrangement as depicted in Fig. 1. The projector projects a sinusoidal fringe pattern onto the object surface. The camera captures the distorted fringe pattern, which is digitally processed, e.g., via Fourier Transform Profilometry (FTP) [1], to obtain the 3D shape of the object.

A captured sinusoidal fringe pattern can be expressed in the complex form as follows,

$$g(x, y) = a(x, y) + c(x, y) \exp\{2\pi i f(x, y)\} + c^*(x, y) \exp\{-2\pi i f(x, y)\}, \quad (1)$$

where

$$c(x, y) = \frac{1}{2} b(x, y) \exp\{i\varphi(x, y)\}, \quad (2)$$

$a(x, y)$ represents the background illumination, $b(x, y)$ relates to the contrast of the fringes, $f(x, y) = f_x x + f_y y$ denote the carrier frequency measured in the x and y directions and $\varphi(x, y)$ is the phase modulation resulting from the object height distribution. $*$ denotes the complex conjugate of $c(x, y)$. A 2D Fourier transform on Eq. (1) yields

$$G(f_x, y) = A(\xi_x, \xi_y) + C(\xi_x - f_x, \xi_y - f_y) + C^*(\xi_x + f_x, \xi_y + f_y), \quad (3)$$

where $A(\xi_x, \xi_y)$ and $C(\xi_x - f_x, \xi_y - f_y)$ are the 1-D Fourier transforms of $a(x, y)$ and $c(x, y)$, respectively.

Fourier transform is well suited for the analysis of signal composed of sinusoidal components as long as $\varphi(x, y)$, $a(x, y)$, and $b(x, y)$ are slowly varying or space invariant. If

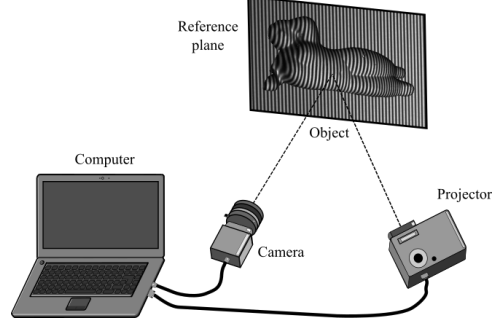


Fig. 1: Fringe projection system.

this condition is fulfilled, a proper band-pass filter can be applied to select $C(\xi_x - f_x, \xi_y - f_y)$. However, in practice, fringe patterns are usually space-varying. These patterns represent nonstationary signals and a description of such signals in the frequency domain by simple Fourier transform provide errors brought on when $C(\xi_x - f_x, \xi_y - f_y)$ superposes on the zero frequency component or higher order spectral components. Consequently, in this case, an appropriate filter must be designed to retain utmost information from $C(\xi_x - f_x, \xi_y - f_y)$ and keep it apart from the background spectrum and others unwanted contributions. If the zero frequency component and the high order spectra component interfere with the useful fundamental spectra, the reconstruction precision will decrease greatly.

Lin *et al* proposed the Hanning window to separate the height information in FTP [2]. However, when dealing with frequency aliasing between the zero-order spectrum and the fundamental spectrum, this approach is not effective to address the band-pass filtering problem [3]. To overcome this difficulty various space-frequency analysis techniques based on Fourier have been proposed. These techniques include windowed Fourier [4] or Gabor transform [5], wavelet transform [6], and smoothed space-frequency distribution [7]. A major restriction of these methods is their non-adaptive nature. *A priori* knowledge of parameters like filter window width and basis function is necessary for generating desirable outputs. Other authors have proposed quasi-sinusoidal projection and π -phase shifting for suppressing the zero frequency component and high-order spectra component [8] and composite stripe projection technology for eliminating zero frequency component [9] for improving the accuracy and measurement range of FTP. These techniques have their own applications according to the property of the measured objects. For instance, the π -

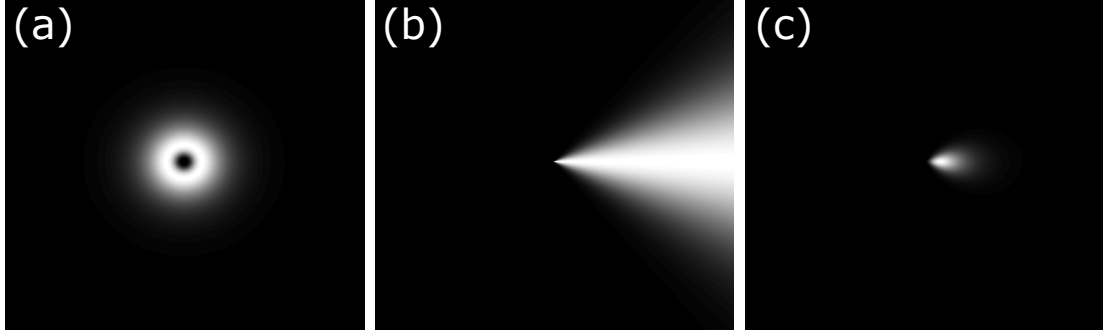


Fig. 2: Log-Gabor filter implementation process. (a) Radial filter with $f_0 = 1/9$ and $\sigma_r = 0.5$ (b) Angular filter with $\theta = 0$ and $\sigma_\theta = \frac{\pi}{5}$. (c) Combination of the radial and angular components to obtain the log-Gabor filter.

shifting technique needs to capture two fringe pattern images with π -phase difference to eliminate the background intensity by a subtracting operation. This improves the accuracy and measurement range but is a clear drawback when measuring dynamic objects and scenes.

Recently, many optimization algorithms, such as Particle swarm optimization (PSO) [10], have been emerged as a new and attractive tool for filter design [11], [12], [13]. The PSO algorithm is well known for it simplicity and computational efficiency, and, unlike other heuristic techniques, this algorithm has a well-balanced mechanism for enhancing the global and local exploration abilities. In view of the developing trend, a new particle swarm optimization approach for filter modeling was developed to achieve more accurate extraction of the first-order spectrum in Fourier Transform Profilometry. The algorithm takes advantage of the adaptive nature of the Log-Gabor filters to model a filter that prevents the zero frequency component and the high order spectra component from interfering with the useful fundamental spectra. Comparing with Hanning filters, log-Gabor filters are designed with an arbitrary bandwidth and for a particular orientation, which is optimized to reduce the over-representation of $C(\xi_x - f_x, \xi_y - f_y)$. Our approach seeks to minimize the presence of phase residues associated with filtering problems. Residues reveal problems in phase retrieval and provide an indication of the difficulty in performing an accurate 3D reconstruction. In the following sections we show the theory and the implementation details, as well as experimental results.

II. LOG-GABOR FILTER

2D Log-Gabor filters are constructed in the polar coordinate system of the frequency domain in terms of two components: radial and angular filters, $H(r, \theta) = H_r(r) \cdot H_\theta(\theta)$, as follows,

$$H(r, \theta) = \exp\left(-\frac{[\log(r/f_0)]^2}{2 \cdot \sigma_r^2}\right) \cdot \exp\left(-\frac{(\theta - \theta_0)^2}{2 \cdot \sigma_\theta^2}\right), \quad (4)$$

where (r, θ) represents the polar coordinates, f_0 is the central frequency, θ_0 is the orientation angle, σ_r is the standard deviation of the radial filter and σ_θ is the standard deviation of the angular filter. σ_r and σ_θ determinate the scale and angular bandwidth, respectively.

Fig. 2 illustrates the log-Gabor filter implementation process in frequency domain. The radial and angular filters area shown in Fig. 2(a) and 2(b), respectively. The two components are combined to obtain the overall log-Gabor filter shown in Fig 2(c).

III. PSO-BASED PARAMETER ESTIMATION

Particle Swarm Optimization (PSO) is an evolutionary optimization technique motivated by the behavior of organisms such as fish schooling and bird flocking. This algorithm has proven its effectiveness for solving optimization problems featuring nonlinearity and high dimensionality reaching good solutions with a minimal parameterization. The PSO algorithm is considered as stochastic optimization method since it initializes with a population of random solutions, called particles. Each particle represents a candidate solution to the optimization problem [14]. These particles change their positions by flying throughout the multi-dimensional search space by following the current optimum particles. This process is performed until the stopping criterion is achieved.

But why particle swarm? A vector of D dimension in search space is a point in a high-dimensional Cartesian coordinate system. As the points move around space testing new parameter values, we can consider each point as a particle. Because all of this particles have this behavior simultaneously and because they tend to cluster together in optimal regions of the search space, they are referred to as a particle swarm [10].

The PSO algorithm has some features that are important to discuss:

- Due to particles only dependence to the objective function to guide the search, this function must be defined from the start, before the initialization of the PSO algorithm.
- A vector of D dimensions represents to one particle, which is a candidate solution of evaluating non-linear system parameters. The dimension D is given by the variables number of the problem to optimize. Through n iterations we call $x_{i,d}$ to position of the i -th particle in the dimension d in such way that we will have $x_i(n) = [x_{i,1}(n) \ x_{i,2}(n) \ \dots \ x_{i,d}(n)]$.
- It is necessary to define a search space. For this is important to limit the problem space setting the minimum x_{min} and maximum x_{max} position that each particle can

have. Being x_{min} the vector with the minimum adjusted position and x_{max} the vector with the maximum set position. In this way, we convert the infinite space of problem in one defined space called search space.

- It is important to define the velocity with which particles will move around the search space, of this parameter depends that there is a good exploration by the particles in the search space. The velocity is a D dimensional vector (like particles) that through n iterations we call $v_{i,d}$ to velocity of the i -th particle in the dimension d in such a way that we will have $v_i(n) = [v_{i,1}(n) v_{i,2}(n) \dots v_{i,D}(n)]$.
- The individual best is the best position in which one particle has been through all iterations. Then, for n iterations $pb_{i,d}$ is the best position related with the best objective function value respect to a position of the i -th particle in the dimension d . Being $pb_i(n) = [pb_{i,1}(n) pb_{i,2}(n) \dots pb_{i,D}(n)]$.
- The global best gb is the best position taking into account all the individual best position $pb_{i,d}$ achieved so far.

A. Objective Function

Once the deformed fringe pattern is 2-D Fourier transformed, the resultant spectrum is filtered by a 2-D log-Gabor filter defined by Eq. (4). The inverse Fourier Transform is applied to the filtered component, and a complex signal is obtained

$$\tilde{c}(x, y) = \frac{1}{2}b(x, y) \exp\{i(2\pi f(x, y) + \varphi(x, y))\} . \quad (5)$$

From Eq. (5), the phase can be solved for by,

$$\varphi(x, y) = \tan^{-1}\left(\frac{\Im[\tilde{c}(x, y)]}{\Re[\tilde{c}(x, y)]}\right) , \quad (6)$$

where $\Re[\tilde{c}(x, y)]$ and $\Im[\tilde{c}(x, y)]$ denote the imaginary and real part of $\tilde{c}(x, y)$, respectively. The arctangent can be considered as a 2π modulus wrapping operator. Therefore the values of the phase $\varphi(x, y)$ range from $-\pi$ to $+\pi$. The obtained phase $\phi(x, y)$ is called the *wrapped* phase map.

As previously discussed, the proposed algorithm seeks for minimizing the presence of phase residues in $\varphi(x, y)$. The residue calculation process can be understood by examining the array in Fig. (3), which contains samples of a wrapped phase function $\varphi(x, y)$. The phase values are in units of 2π rad and the residues are depicted as a green box for a negative residue and as a red box for a positive one. The phase derivatives are computed discretely as local wrapped two-point wrapped phase differences. The residue charge is obtained by summing the phase differences around the 2×2 pixels closed path as follows [15], [16],

$$\begin{aligned} \mathbf{Q}_{i,j} = \sum_{k=1}^4 \Delta_k &= \mathbb{W}\{\varphi(i+1, j) - \varphi(i, j)\} + \\ &\quad \mathbb{W}\{\varphi(i+1, j+1) - \varphi(i+1, j)\} + \quad (7) \\ &\quad \mathbb{W}\{\varphi(i, j+1) - \varphi(i+1, j+1)\} + \\ &\quad \mathbb{W}\{\varphi(i, j) - \varphi(i, j+1)\} , \end{aligned}$$

where (i, j) relates to the pixel index and \mathbb{W} is the wrapping operator that wraps the phase differences into the interval $(-\pi, \pi]$. Finally, our objective function is given by

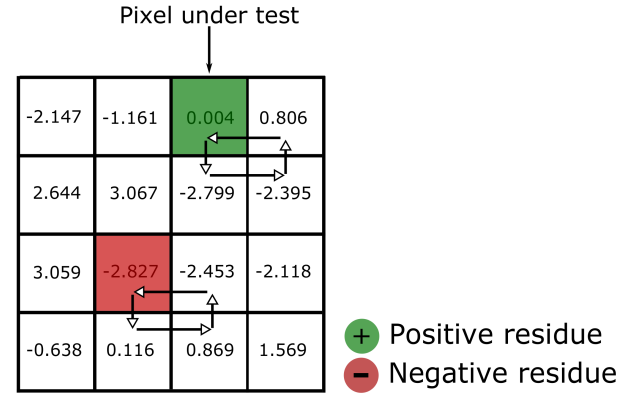


Fig. 3: Typical array of wrapped phase values.

$$NR = \sum_i^m \sum_j^n \mathbf{Q}_{i,j} . \quad (8)$$

Eq. 8 calculates the total number of residues (NR) over the whole wrapped phase array. Our approach focuses on finding the log-Gabor filter's optimal parameters θ_0 , σ_r and σ_θ in such way that the residues number is minimized.

B. Particles

To find the minimum of the above objective function, we will use a total of 10 particles. As explained above a particle, which is a candidate solution of evaluating non-linear system parameters, can be represented as a vector of D dimensions. In this case, the dimension D is the parameters number of the filter to implement.

C. Velocity updating $v_{i,d}(n+1)$

The velocity update, which is the velocity for the next iteration, is the sum of three components given for the following equation:

$$\begin{aligned} v_{i,d}(n+1) = v_{i,d}(n) &+ \\ &c_1 r_1 [pb_{i,d}(n) - x_{i,d}(n)] + \\ &c_2 r_2 [gb_d(n) - x_{i,d}(n)] . \quad (9) \end{aligned}$$

The first component $v_{i,d}(n)$ is the velocity in the actual iteration. The second term $c_1 r_1 [pb_{i,d}(n) - x_{i,d}(n)]$ is the cognitive component, that depend of acceleration constant c_1 , is related with the particle distance with its best visited position. The third element $c_2 r_2 [gb_d(n) - x_{i,d}(n)]$ is the social component, that depend of acceleration constant c_2 , and is related with the distance between particle and the global best position. Finally the constants r_1 and r_2 are two uniformly random numbers between 0 and 1.

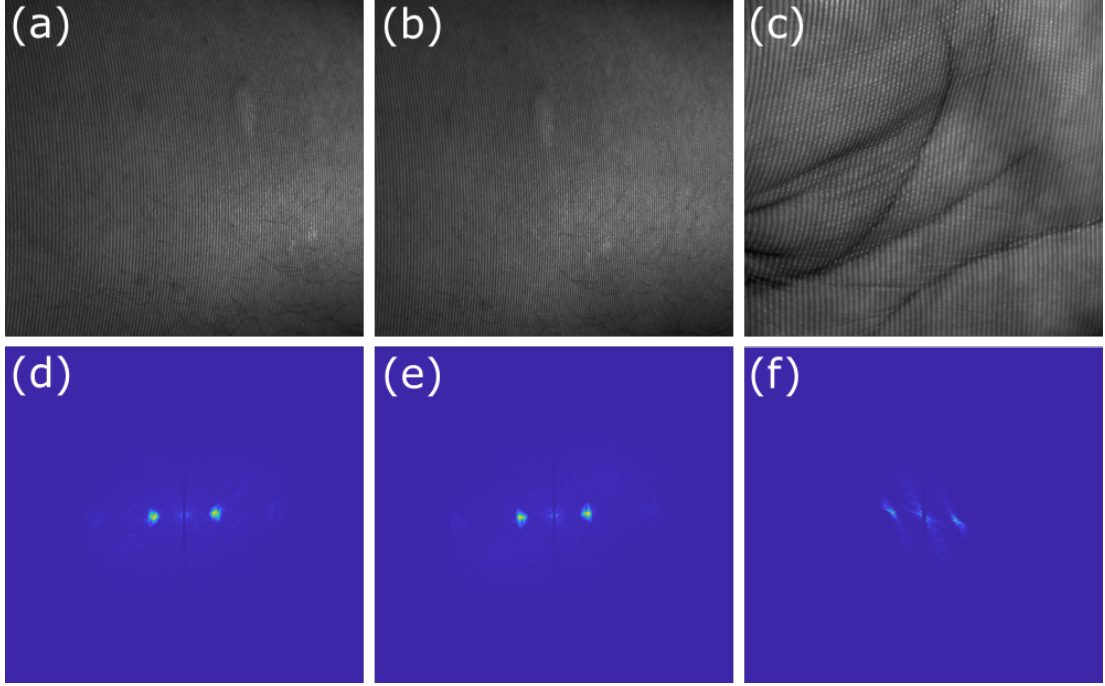


Fig. 4: Tested fringe images. (a) I_1 . (b) I_2 . (c) I_3 . (d) Fourier transform magnitude spectra of I_1 , (e) I_2 and (f) I_3 .

D. Position updating $x_{i,d}(n+1)$

Once calculated the velocity $v_{i,d}(n+1)$ of each particle, we must find its respective positions for the next iteration. Then the next particles position is described as follows

$$x_{i,d}(n+1) = x_{i,d}(n) + v_{i,d}(n+1) . \quad (10)$$

IV. EXPERIMENTS AND RESULTS

In order to prove the effectiveness of the proposed method, we have selected three fringe images I_1 , I_2 , and I_3 , shown in Fig. 4(a), 4(b) and 4(c), respectively. The resultants complex spectrum, by applying Fourier transform to I_1 , I_2 , and I_3 , are respectively shown in Fig. 4(d), 4(e), and 4(f). In order to effectively achieve our goal we took into account the following considerations:

- Our objective function is given by Eq. 8.
- We have chosen a total of 10 particles for the algorithm.
- The principal parameters for the Log-Gabor filter, given by Eq. 4, were set as follow: f_0 is fixed to a specific value of 1/20. This variable does not enter into the optimization process. σ_r ranges between [0.75, 0.85], σ_θ ranges between [0.1, 0.4], and θ_0 ranges between [-0.3491, 0.3491]. In based on the above we have that $x_{min} = [0.75, 0.1, -0.3491]$ and $x_{max} = [0.85, 0.4, 0.3491]$.
- The maximum velocity of particles was set to 0.1.
- According to the exposed in [17], acceleration coefficients for cognitive and social component were taken as $c_1 = c_2 = 2.05\chi$, where $\chi = 0.72984$.
- Finally, the maximum number of Iterations was fixed to 10.

These parameters were all used for the three test images, except for the fringe pattern in Fig. 4(c) for which the range of θ_0 ranges between [0.0175, 0.3491].

Table I shows the results obtained by applying the traditional Hanning window filter and the proposed PSO-based Log-Gabor filter to I_1 , I_2 , and I_3 . NR_H and NR_G denote the number residues obtained for Hanning window filter and the PSO-based Log-Gabor filter, respectively. gb_{σ_r} , gb_{σ_θ} , and gb_θ are the global best position for σ_r , σ_θ and θ , considering all the individual best position $pb_{i,d}$ achieved so far. Some illustrative examples of these data are shown in Fig. 5. Each row shows (from top to bottom) the results for I_1 , I_2 , and I_3 . Each column shows (from left to right) the applied Hanning window filters, the wrapped phase maps obtained by Hanning filtering, the optimized log-Gabor filters and the resultant wrapped phase map after applying the log-Gabor filter. On the basis of these results, we appreciate the effectiveness of the proposed for removing phase residues introduced during the filtering stage. As shown in Table I, in all cases PSO-gabor filter significantly reduces the number of residues in the wrapped phase maps. On the other hand, using hanning filter, the number of phase residues increases since it generates overestimation of the main frequency component. This produces the filtering of frequencies that are not related to the three-dimensional shape information of the studied object. Since Fourier transform profilometry is based on filtering for obtaining the fundamental frequency spectrum in the frequency domain, the frequency aliasing between the fundamental spectrum and all other spectra has great influence on the measurement accuracy and measurable slope of height variation.

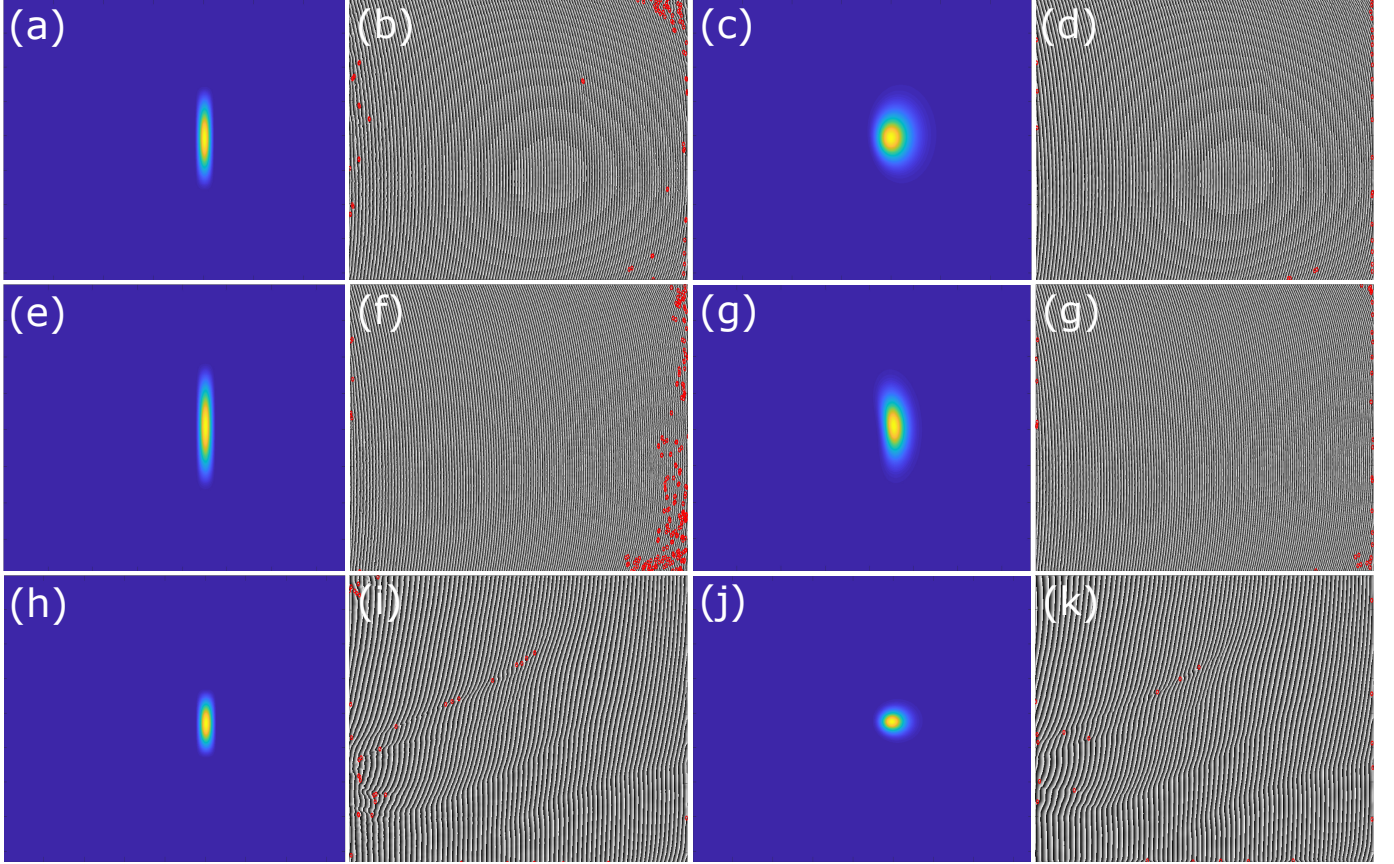


Fig. 5: Illustrative results. Each row shows (from top to bottom) the results for the fringe images I_1 , I_2 , and I_3 in Fig. 4. Each column shows (from left to right) the applied Hanning window filters, the wrapped phase maps obtained by Hanning filtering, the optimized log-Gabor filters and the resultant wrapped phase map after applying the log-Gabor filter.

TABLE I: Results obtained with Hanning and PSO Gabor filter

	I_1	I_2	I_3
NR_H	80	204	40
NR_G	29	36	21
gb_{σ_r}	0.7844	0.8428	0.8450
gb_{σ_θ}	0.2352	0.2671	0.1655
gb_θ	-0.2558	-0.1893	-0.1468

V. CONCLUSIONS

In this work we have developed a new particle swarm optimization approach for log-Gabor filters modeling to achieve more accurate extraction of the first-order spectrum in Fourier Transform Profilometry. Results shows the effectiveness of the proposed for removing phase residues introduced during the filtering stage. In all cases PSO-base log-Gabor filter significantly reduces the number of residues in the obtained wrapped phase maps. Future efforts related to this topic will be aimed at reducing the computational cost of the proposed method.

REFERENCES

- [1] M. Takeda, H. Ina, and S. Kobayashi, “Fourier-transform method of fringe-pattern analysis for computer-based topography and interferometry,” *JosA*, vol. 72, no. 1, pp. 156–160, 1982.
- [2] J. F. Lin and X. Su, “Two-dimensional Fourier transform profilometry for the automatic measurement of three-dimensional object shapes,” *Optical Engineering*, vol. 34, no. 11, pp. 3297–3302, 1995.
- [3] R. Vargas, J. Pineda, A. G. Marrugo, and L. A. Romero, “Background intensity removal in structured light three-dimensional reconstruction,” in *Signal Processing, Images and Artificial Vision (STSIVA), 2016 XXI Symposium on*. IEEE, 2016, pp. 1–6.
- [4] Q. Kemao, “Windowed fourier transform for fringe pattern analysis,” *Applied Optics*, vol. 43, no. 13, pp. 2695–2702, 2004.
- [5] J. Zhong and J. Weng, “Dilating gabor transform for the fringe analysis of 3-d shape measurement,” *Optical Engineering*, vol. 43, no. 4, pp. 895–899, 2004.
- [6] ———, “Spatial carrier-fringe pattern analysis by means of wavelet transform: wavelet transform profilometry,” *Applied optics*, vol. 43, no. 26, pp. 4993–4998, 2004.
- [7] A. Federico and G. H. Kaufmann, “Phase retrieval in digital speckle pattern interferometry by use of a smoothed space-frequency distribution,” *Applied optics*, vol. 42, no. 35, pp. 7066–7071, 2003.
- [8] X. Su and W. Chen, “Fourier transform profilometry:: a review,” *Optics and Lasers in Engineering*, 2001.
- [9] C. Guan, L. Hassebrook, and D. Lau, “Composite structured light pattern for three-dimensional video,” *Optics Express*, vol. 11, no. 5, pp. 406–417, 2003.
- [10] J. Kennedy, “Particle swarm optimization,” in *Encyclopedia of machine learning*. Springer, 2011, pp. 760–766.
- [11] N. Karaboga, “A new design method based on artificial bee colony algorithm for digital iir filters,” *Journal of the Franklin Institute*, vol. 346, no. 4, pp. 328–348, 2009.
- [12] N. He, D. Xu, and L. Huang, “The application of particle swarm optimization to passive and hybrid active power filter design,” *IEEE*

- transactions on industrial electronics*, vol. 56, no. 8, pp. 2841–2851, 2009.
- [13] Y.-P. Chang, “Integration of sqp and pso for optimal planning of harmonic filters,” *Expert Systems with Applications*, vol. 37, no. 3, pp. 2522–2530, 2010.
 - [14] Y.-L. Lin, W.-D. Chang, and J.-G. Hsieh, “A particle swarm optimization approach to nonlinear rational filter modeling,” *Expert Systems with Applications*, vol. 34, no. 2, pp. 1194–1199, 2008.
 - [15] D. C. Ghiglia and M. D. Pritt, *Two-dimensional phase unwrapping: theory, algorithms, and software*. Wiley New York, 1998, vol. 4.
 - [16] D. J. Bone, “Fourier fringe analysis: the two-dimensional phase unwrapping problem,” *Applied optics*, vol. 30, no. 25, pp. 3627–3632, 1991.
 - [17] D. Bratton and J. Kennedy, “Defining a standard for particle swarm optimization,” in *Swarm Intelligence Symposium, 2007. SIS 2007. IEEE*. IEEE, 2007, pp. 120–127.